Journal of Thermal Analysis and Calorimetry (2019) 135:2747–2757
https://doi.org/10.1007/s10973-018-7614-z

Incompatible effects of specific acids on the thermokinetics of 1,1-bis(*tert*-butylperoxy)-3,3,5-trimethylcyclohexane

Wei-Chun Chen[1] · Chi-Tang Yeh[2] · Chi-Min Shu[3]

Received: 25 February 2018 / Accepted: 29 July 2018 / Published online: 14 August 2018

Abstract

1,1-Bis(*tert*-butylperoxy)-3,3,5-trimethylcyclohexane (TMCH), an industrial initiator and cross-linking agent comprising two active peroxy bonds, becomes unstable when specific acids—namely phosphoric acid (H_3PO_4), sulfuric acid (H_2SO_4), nitric acid (HNO_3), or hydrochloric acid (HCl)—are added to it. The incompatible reactivity of TMCH with these specific acids was monitored through differential scanning calorimetry (DSC) and thermal activity monitor III (TAM III). Thermophysical parameters, including exothermic onset temperature, decomposition heat, and peak temperature, were estimated through DSC dynamic testing to obtain the exothermic ranking. Isothermal testing was conducted using TAM III to estimate the thermokinetic parameters of the mixture of TMCH and a specific acid. A high reaction enthalpy was observed when TMCH was mixed with H_2SO_4, HNO_3, or HCl due to the characteristic acid-catalyzed reactions. Furthermore, HCl initiated an earlier onset temperature for TMCH decomposition, and the mixtures of TMCH with HNO_3 and HCl presented multiple thermal curves with complex exothermic peaks. In summary, the thermokinetic parameters and reaction models of TMCH with specific acids were evaluated to classify the runaway potential.

Keywords 1,1-Bis(*tert*-butylperoxy)-3,3,5-trimethylcyclohexane (TMCH) · Incompatible reactivity · Acid-catalyzed reactions · Multiple thermal curves · Thermokinetic parameters

List of symbols

C_p	Specific heat capacity (kJ mol^{-1} K)
dT/dt	Self-heating rate (°C min^{-1})
E_a	Apparent activation energy (8.314 J K^{-1} mol^{-1})
k_i	Rate constant ((mol L^{-1})$^{-n+1}$ s^{-1}), i = 1, 2…
k_0	Frequency factor ((mol L^{-1})$^{n-1}$ s^{-1})
$k(T)$	Specific rate constant at temperature T ((mol L^{-1}) $^{-n+1}$ s^{-1})
m	Mass (g)
N	Reaction order (dimensionless)
n_i	Reaction order of the ith stage (dimensionless)
R	Universal gas constant (8.314 J K^{-1} mol^{-1})
Q	Heat flow (W g^{-1})
T	Absolute temperature (°C)
T_0	Apparent exothermic onset temperature (°C)
T_{max}	Maximum temperature (°C)
T_p	Peak temperature (°C)
t	Time (s)
t_0	Initiated time of reaction (s)
t_f	Time of reaction completed (s)
z	Autocatalytic constant (dimensionless)
α	Degree of conversion (dimensionless)
β	Heating rate (°C min^{-1})
ΔH	Enthalpy of reaction (J g^{-1})
ΔH_d	Heat of decomposition (J g^{-1})
[TMCH]	Concentration of TMCH (mol L^{-1})

✉ Chi-Min Shu
shucm@yuntech.edu.tw

[1] Bachelor Program in Interdisciplinary Studies, National Yunlin University of Science and Technology (YunTech), 123, University Rd., Sec. 3, Douliou 64002, Yunlin, Taiwan, ROC

[2] Doctoral Program, Graduate School of Engineering Science and Technology, YunTech, 123, University Rd., Sec. 3, Douliou 64002, Yunlin, Taiwan, ROC

[3] Department of Safety, Health, and Environmental Engineering, YunTech, 123, University Rd., Sec. 3, Douliou 64002, Yunlin, Taiwan, ROC

Introduction

Thermal unstable chemicals, such as organic peroxides (OPs), readily mix with acids, alkalis, or metal ions. However, these unstable chemicals are known

contaminants that cause thermal runaway scenarios when exposed to heat. Even a low concentration of contaminants and low heat accumulation can trigger such a complex heat phenomenon with these chemicals. During this uncontrollable thermal reaction of OPs, a large amount of energy is released, which may result in an explosion [1–3]. The complex heat phenomenon is due to peroxy functional groups, which are crucial for activating an oxidation reaction, and the cleavage of peroxy bonds, which are lightly susceptible to thermal and photolytic reactions, which generate enormous amount of heat [4–9].

Studies have reported that OPs exhibit high thermal sensitivity, catalytic activity, and energetic bonding. Thus, a free radical chain reaction occurs, and the rate of exothermic reaction increases. However, thermally runaway potential may be occurred when OPs were added with incompatible impurities. If a regulative disposal management of such impurities is not adopted, then such mixtures may be formed and thus decomposition reactions may occur. These mixtures formed can react with liberated oxygen molecules and form peroxide solvents, thus leading to a complicated decomposition reaction [10–12]. OPs are a subset of catalytic materials that deserve unusually industrial importance but they also have instability concerns that make them the most thermally decomposing chemicals.

1,1-Bis(tert-butylperoxy)-3,3,5-trimethylcyclohexane (TMCH) is a cross-linking agent used to synthesize styrene and polyethylene and to initiate polymerization, that is, TMCH is used as an activator in process manufacturing. The formation of free radicals induces a rapid autocatalytic decomposition, thus causing an exothermic runaway reaction that is followed by combustion or explosion. TMCH—a highly sensitive, exothermic, and unstable nature with its complex and unstable structures—needs to be fully understood the temperature induced the decomposition and increased exothermic rate. In contrast, contamination initiated decomposition and released hazardous by-products. An appropriate thermal safety evaluation should be applied while preparing, manufacturing, transporting, storing, and discarding. Previous studies have primarily focused on the heat of decomposition and the order of the reaction for pure TMCH [13–15]. The high enthalpy of TMCH causes thermal runaway; simultaneously, the evaporation and gasification processes lead to the formation of unstable by-products. Temperature elevation has a salient accelerating effect on the reaction rate. Hence, when working with TMCH, the temperature should be carefully monitored to avoid initiation of the exothermic reaction. Moreover, the metal-ion-catalyzed reactions of TMCH with $CuCl_2$ and $FeCl_3$ were readily cleaved to the peroxide bond by electron reduction, thus causing high heat flux during thermal decomposition [16–19]. In addition to heat sources and elevated temperatures, contaminants such as rust or metal ions can initiate thermal decomposition of TMCH and accelerate thermal runaway reactions.

An unexpected exothermic reaction is one of the most common hazards, which could be prevented if the exothermic mechanisms are clearly understood. Thermal analysis is crucial to improve the safety management for TMCH. To classify the thermal hazards that occur when strong acids are mixed with TMCH, we evaluated thermal decomposition characteristics and acid-catalyzed reactions when TMCH reacted with four acids separately—phosphoric acid (H_3PO_4), sulfuric acid (H_2SO_4), nitric acid (HNO_3), or hydrochloric acid (HCl). Furthermore, dynamic scanning calorimetry (DSC) and isothermal calorimetry tests were conducted to analyze the thermal decomposition characteristics and various acid-catalyzed hazards. Ionic acids have a tendency to donate hydrogen ions during reactions in which heat and gases are generated. The kinetic variables in the acid-catalyzed reactions of TMCH were crucial in determining the rate of a reaction. The enthalpy (such as the heat of decomposition) and the reaction rate determine the rate of heat released; this released heat must be monitored to control the incompatible behaviors of TMCH. Both calorimeters, DSC and thermal activity monitor III (TAM III), were used to calculate the dynamic heat flow (Q), apparent onset temperature (T_0), time to maximum rate under an isothermal conditions (TMR_{iso}), and reaction induced period (t_i). The kinetic data, such as apparent activation energy (E_a), frequency factor (k_0), and reaction order (N) of TMCH under various isothermal conditions during acid-catalyzed decomposition, were evaluated using TAM III. On the basis of these results, thermokinetic models were developed to determine the reaction rate of TMCH with the aforementioned acids and the influence of impurities on the reaction rate.

Experimental

Materials

In the present study, commercial-grade TMCH (ACE Chemical Corp., Taiwan; 88.0 mass%) and various specific acids (H_3PO_4, H_2SO_4, HNO_3, and HCl) were used as the reaction media to assess the thermal reactions and associated thermokinetic parameters. Moreover, when ionizing acids or oxidizing agents are present in a reaction, free radicals can be generated in bulk and at a rapid enough pace for the reaction to be violent. The normality of the specific acids was maintained at an equivalent concentration of 6.0 N to analyze the thermal compatibility of TMCH.

Differential scanning calorimetry

Temperature-programmed screening experiments were conducted using a Mettler TA8000 system coupled with a DSC821^e measuring cell [20] in the range 30.0–300.0 °C and at heating rates of 0.5, 1.0, 2.0, 4.0, 8.0, and 10.0 °C min^{-1} for dynamic thermal heating. The programmable temperature-control system applied in the DSC system realized heating and cooling temperature from 0.01 to 100.0 °C and detected the temperature range of a target sample in the range − 150.0 to 700.0 °C. The sample was loaded and sealed in a gold-plated, high-pressure crucible (Mettler ME-26732) that could withstand pressure up to 15.0 MPa. The thermal curves were obtained using the STAR^e thermal analysis software to evaluate the thermal decomposition behaviors of the sample. The temperatures of the reference sample and target sample varied differently because the target sample released energy during thermal decomposition, which resulted in heat generation in the cell. Therefore, the temperatures in the reference sample and target sample cells were not equal after the heating test. Moreover, dynamic temperature-programmed screening was conducted to estimate the apparent onset temperature (T_0), peak temperature (T_p), maximum temperature (T_{max}), and heat of decomposition (ΔH_d) and to obtain an estimated reaction profile.

Thermal activity monitor III

TAM III, an isothermal calorimeter, is a thermally sensitive and dedicated stability-detecting device that can detect in the temperature range 5.0–150.0 °C and can be used in numerous domains, such as pharmaceuticals, material and life sciences, and physical chemistry [21–22]. The average temperature fluctuation of TAM III is ± 10 μK, and the drift over 24 h is within ± 100 μK. The stability of the TAM III thermostat provides a pseudo-perfect environment for isothermal and temperature scanning measurements (microcalorimeter). In this study, mineral oil was used in the thermostat of TAM III to warrant chemical and physical equilibrium [24, 23]. The injection of each sample in an ampoule contained 100.0 mg of TMCH with 10.0 mg of H_3PO_4, H_2SO_4, HNO_3, or HCl. The calorimetric screening was used by TAM III to evaluate the exothermic behaviors of 88.0 mass% TMCH and 88.0 mass% TMCH that were reacted with four selected specific acids under isothermal conditions at 60.0, 70.0, 80.0, and 90.0 °C.

Kinetics treatment and reaction model evaluation

Thermal Safety Software (TSS) was used (TDPro and ForK) to simulate the *N*-th order reaction, autocatalytic reaction, and thermokinetic parameters. The crucial step while simulating the amplification process is the selection of the thermokinetic model. These models can be applied to reduce thermal hazards and enhance the safety of a system of interest [24]. Thermokinetic models were developed on the basis of specific properties of chemical reactions. The properties were obtained using experimental data of distinct material structures. Moreover, the thermokinetic parameters of chemical reactions were computed.

The thermokinetics of a material can be classified as single or multistage reactions and divided into independent, parallel, and continuous stages that are described using the Arrhenius equation with reaction conversion functions $f(\alpha)$, as presented as follows [25, 26].

A simple concentration change of TMCH for the degree of conversion (α) is related to the ratio in a period of time (t):

$$[\mathrm{TMCH}]_t = [\mathrm{TMCH}]_0 \cdot (1-\alpha). \tag{1}$$

The concentration reduction rate of TMCH during self-decomposition or catalytic reaction can be expressed using the following simplified *N*-th order equation:

$$\frac{\mathrm{d}[\mathrm{TMCH}]}{\mathrm{d}t} = -k(T)\cdot[\mathrm{TMCH}]^n \cdot f(\alpha). \tag{2}$$

For a normal chemical reaction rate:

$$k(T) = k_0 \cdot \exp\left[\frac{-E_a}{RT}\right]. \tag{3}$$

For the *N*-th model, $A \overset{k1}{\Rightarrow} B$.

$$\text{Thus,}\quad f(\alpha) = (1-\alpha)^{n_i}. \tag{4}$$

For the autocatalytic model, $A \overset{k_1}{\Rightarrow} B$ and $A + B \overset{k_2}{\Rightarrow} 2B$.

$$\text{Thus,}\quad f(\alpha) = (1-\alpha)^{n_i}\cdot\alpha^z. \tag{5}$$

$$\frac{(1-\alpha)}{\alpha} = \frac{n_i}{z}. \tag{6}$$

The variations in the TMCH concentration and degree of conversion $f(\alpha)$ for an *N*-th order reaction by using the thermal analysis technique can be described as follows:

$$f(\alpha) = \frac{\Delta H}{\Delta H_d} = \frac{\int_{t_0}^{t} Q\mathrm{d}t}{\int_{t_0}^{t_f} Q\mathrm{d}t}, \quad 0 \le \alpha \le 1. \tag{7}$$

By combining the thermal analytic solutions with result of Arrhenius kinetic equation, the reciprocal of the self-

heating rate can be obtained, which is the principle of DSC [12]. The self-heating rate was estimated using the DSC data of the physical–chemical properties and the TSS kinetic simulation data. The kinetics of the reaction was estimated by substituting the self-heating rate ($dT\,dt^{-1}$) in a computing program. The variations in the self-heating rate of TMCH could be calculated as follows by applying the Arrhenius kinetic model, which yields a simplified thermal analytic solution for the self-heating rate:

$$\left(\frac{dT}{dt}\right)_{TMCH} \cong \frac{\Delta H_d}{m \cdot c_p} \cdot k(T) \cdot [TMCH]^n \cdot f(\alpha) = \Delta T \cdot k_0 \cdot \exp\left[\frac{-E_a}{R \cdot T}\right] \cdot [TMCH]^n \cdot f(\alpha). \quad (8)$$

Results and discussion

Thermal dynamic analysis using DSC tests

The DSC experimental results of dynamic thermal heating program were acquired by thermal spectrum analysis to reveal energy release or heat of decomposition, apparent onset temperature to initiate an exothermic reaction, and thermophysical data. Table 1 and Fig. 1 display the experimental data and thermal curves of pure TMCH decomposing at various heating rates of 0.5, 1.0, 2.0, 4.0, and 8.0 °C min^{-1} using DSC dynamic program. A chemical is considered to be hazardous when the heat of decomposition exceeds 200 J g^{-1} due to the thermal instability of the chemical. One exothermic peak was observed when TMCH decomposed at elevated temperatures. In addition, the calorimetric testing results for TMCH mixing with four specific acids, which being the acidic stimuli, are listed in Table 2 and Fig. 2. An earlier T_0 was initiated when TMCH reacted with HNO_3 or HCl; additionally, for the case in which TMCH reacting with HNO_3 has a relatively high exothermic peak after the first exothermic peak. The steepest exothermic peak emerged as TMCH was added with H_2SO_4 at a higher temperature. The thermal curves are similar on both pure TMCH and TMCH added with H_3PO_4 illustrating that the acid-catalyzed effect of H_3PO_4 in TMCH was insignificant. Most acid-catalyzed decompositions for TMCH and acidic stimuli evidently resulted in violent exothermic hazards.

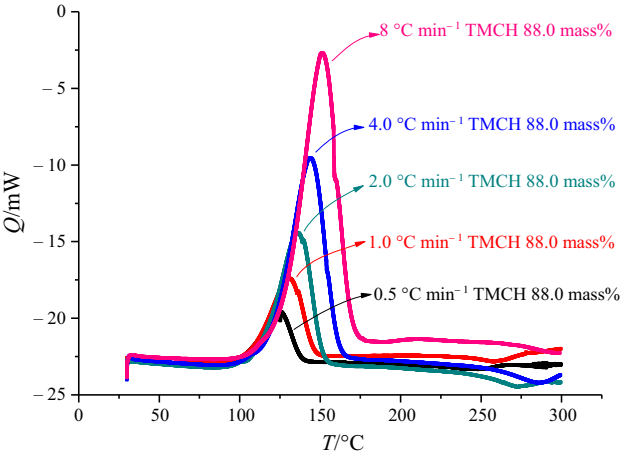

Fig. 1 Thermal curves of heat flow versus temperature for 88.0 mass% TMCH decomposition at various heating rates of 0.5, 1.0, 2.0, 4.0, and 8.0 °C min^{-1} by DSC dynamic heating program

Table 2 Calorimetric data obtained from the dynamic heating experiments of 88.0 mass% TMCH and its mixture of 6.0 N H_3PO_4, H_2SO_4, HNO_3, or HCl conducted by DSC

Tested chemicals	Mass/mg	T_0/°C	T_p/°C	ΔH_d/kJ mol^{-1}
TMCH	4.0	121.3	145.1	1288
TMCH + H_3PO_4	2.9 + 1.1	123.4	148.0	1399
TMCH + H_2SO_4	2.8 + 1.0	119.0	121.1	1783
TMCH + HNO_3	3.1 + 1.0	54.6	117.6	1720
TMCH + HCl	3.1 + 1.0	52.7	64.1	1646

Isothermal scanning test performing by TAM III

To assess the nature of induction time of reactive materials, equilibrium at the test temperature is of more importance to the quality of the isothermal data. Incompatibility testing is able to recognize hazards associated with gross impurities or characteristic reactions in a short-time frame. As for the thermokinetic parameters, such as TMRiso and maximum heat flow, they were computed using TAM III. TMR_{iso} was employed to appraise the emergency response and

Table 1 Calorimetric data obtained from the dynamic heating experiments of 88.0 mass% TMCH conducted by DSC at 0.5, 1.0, 2.0, 4.0, and 8.0 °C min^{-1}

Sample	Mass/mg	β/°C min^{-1}	T_0/°C	T_p/°C	T_{max}/°C	ΔH_d/J g^{-1}
TMCH	6.9	0.5	101.6	125.7	142.2	1219
	6.0	1.0	113.3	130.6	151.6	1212
	5.0	2.0	116.4	136.1	157.5	1276
	4.0	4.0	121.3	144.1	167.0	1288
	2.9	8.0	127.0	151.3	175.4	1297

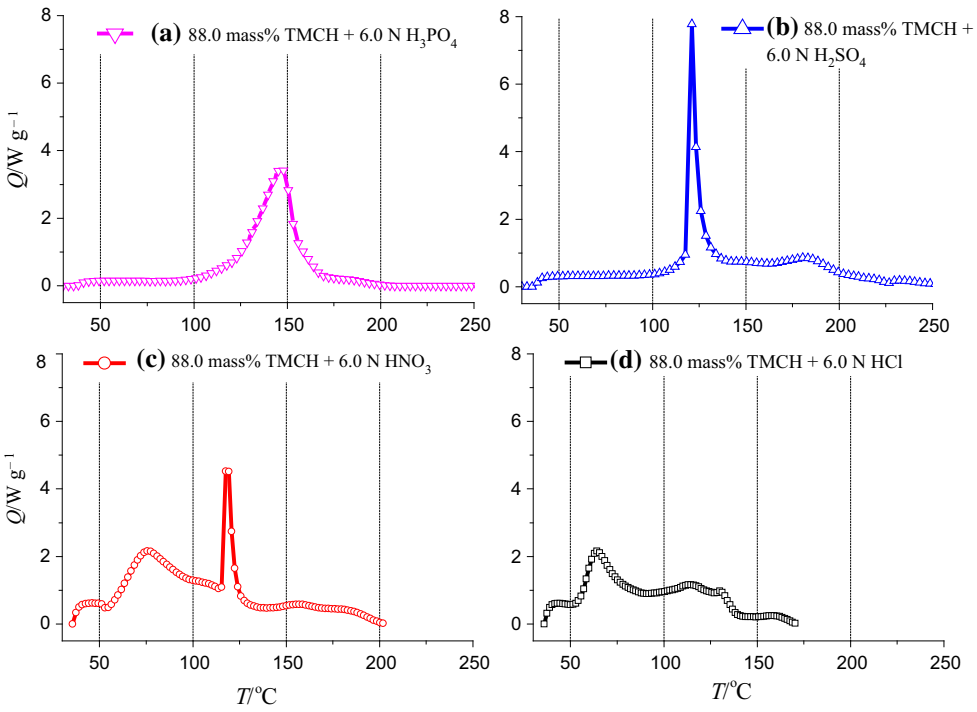

Fig. 2 Thermal curves of heat flow versus temperature for the decomposition of 88.0 mass% TMCH added with various acids of **a** H_3PO_4, **b** H_2SO_4, **c** HNO_3, and **d** HCl at a heating rate of 4.0 °C min^{-1} by DSC dynamic heating program

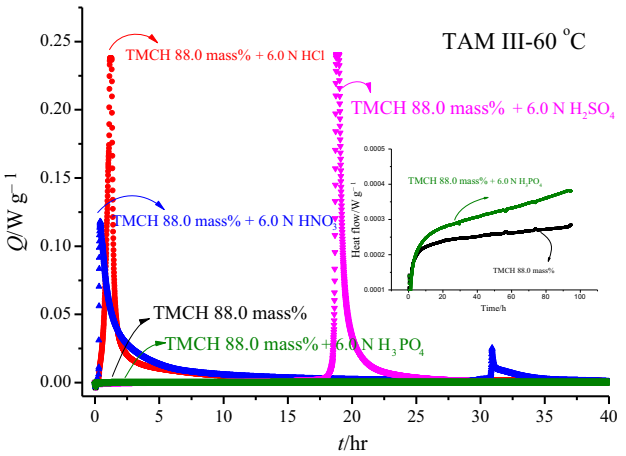

Fig. 3 Isothermal curves of heat flow versus time for 88.0 mass% TMCH and its mixtures of 6.0 N H_3PO_4, H_2SO_4, HNO_3, or HCl at 60.0 °C by TAM III

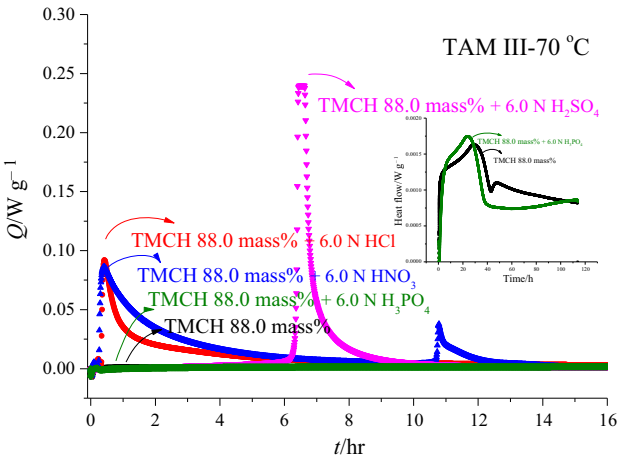

Fig. 4 Isothermal curves of heat flow versus time for 88.0 mass% TMCH and its mixtures of 6.0 N H_3PO_4, H_2SO_4, HNO_3, or HCl at 70.0 °C by TAM III

induction time in the TMCH bulk storage, and heat flow could trace the variation of enthalpy with temperature and time. Figures 3–6 delineate the TMR_{iso} of TMCH and of the mixture of TMCH and H_3PO_4, H_2SO_4, HNO_3, or HCl. When TMCH added with H_2SO_4, HNO_3, or HCl at the isothermal conditions of 60.0, 70.0, 80.0, and 90.0 °C, TMR_{iso} was completed finished no more than 24 h. Moreover, the maximum heat flow increased significantly with temperatures when TMCH was added with the acids but minimized the TMR_{iso}. Heat flow and TMR_{iso} of TMCH and of the mixture of TMCH and H_3PO_4 were insignificant because of unsustainable energy to induce thermal decomposition of TMCH among our test temperatures. Both HNO_3 and HCl might be hazardous stimuli for the acid-catalyzed decomposition of TMCH. Figures 3–6 show the thermal decomposition of pure TMCH and TMCH added with the selected strong acids at various isothermal temperatures 60.0, 70.0, 80.0, and 90.0 °C executed by TAM III tests.

When TMCH was added with 6.0 N of HNO_3 or HCl, the heat flow initiated earlier than other acids at 60.0 °C; similar trends were surveyed for decompositions at 70.0, 80.0, and 90.0 °C. In addition, two exothermic peaks in

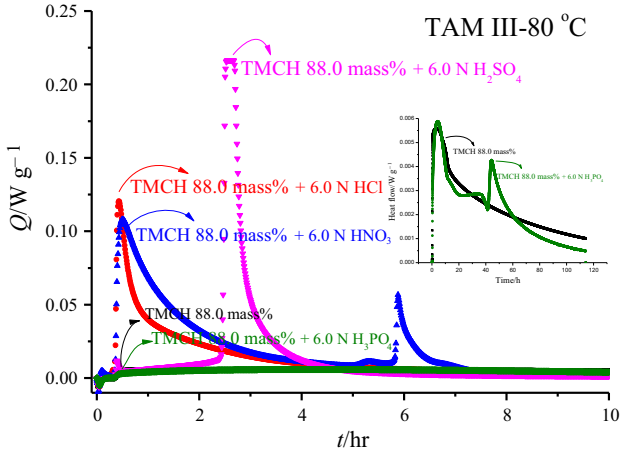

Fig. 5 Isothermal curves of heat flow versus time for 88.0 mass% TMCH and its mixtures of 6.0 N H_3PO_4, H_2SO_4, HNO_3, or HCl at 80.0 °C by TAM III

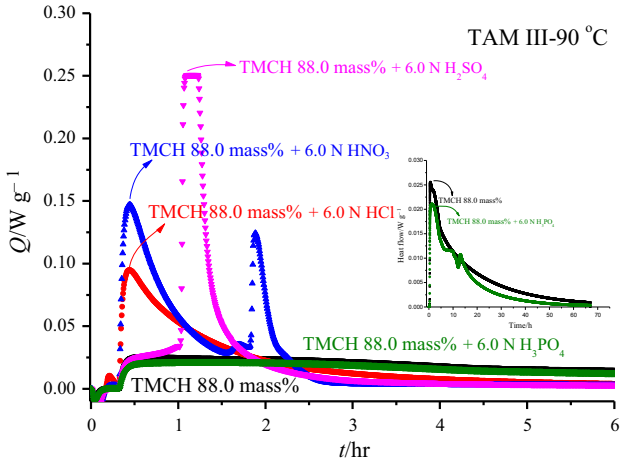

Fig. 6 Isothermal curves of heat flow versus time for 88.0 mass% TMCH and its mixtures of 6.0 N H_3PO_4, H_2SO_4, HNO_3, or HCl at 90.0 °C by TAM III

DSC curves were observed in the set of experiments when TMCH was added with 6.0 N HNO_3, along with the dynamic heating results of DSC. The TMCH-HNO_3 decomposition illustrated two exothermic peaks, in which the first peak occurred within a half an hour in the testing temperatures; furthermore, the second one has higher heat flow and induced earlier at an isothermal scanning of 90.0 °C. Therefore, the decomposition of TMCH added with 6.0 N HNO_3 released a substantial amount of heat, which had a significant thermal hazard of the acid-catalyzed reaction. From the isothermal testing in Fig. 6, TMCH adding with all acids have shown that the obviously thermal decomposition induced higher than 90 °C. Exothermic peakswere observed that TMCH adding with HNO_3 or HCl induced exothermic potential even at 60.0 °C under a storage condition.

Thermal behaviors of the autocatalytic reaction and the *N*-th order reaction

The kinetics of an exothermic reaction is able to assess the runaway potential of the reactive substance. ASTM standard E698 on thermal stability kinetics calls for determination of kinetic parameters by the peak temperature method which requires the measurement of reaction peak temperature as a function of linear-programmed heating rate [11, 17, 27]. To calculate a value for the apparent activation energy E_a and k_0, the estimation is used as follows:Ozawa method:

$$\log(\beta) = \log\frac{k_0 \cdot E_a}{R} - 2.315 - 0.4567\frac{E_a}{R \cdot T_p}. \tag{9}$$

Kissinger method:

$$\ln\left(\frac{\beta}{T_p^2}\right) = \ln\frac{k_0 \cdot R}{E_a} - \frac{E_a}{R \cdot T_p}. \tag{10}$$

Linear regression of the plots is conducted to measure E_a (slope) and k_0 (intercept):

$$\begin{aligned} &\text{Slope}: -0.4567\frac{-E_a}{R}(\text{Ozawa}) \quad \text{or} \\ &\frac{-E_a}{R} = \frac{\mathrm{d}\left[-\ln\left(\frac{\beta}{T_p^2}\right)\right]}{\mathrm{d}\left(\frac{1}{T_p}\right)}(\text{Kissinger}), \end{aligned} \tag{11}$$

$$\begin{aligned} &\text{Intercept}: k_0 = \frac{10^{\beta+2.315} \cdot \mathrm{R}}{E_a}(\text{Ozawa}) \quad \text{or} \\ &k_0 = \frac{\beta \cdot E_a}{T_p^2 \cdot R}(\text{Kissinger}). \end{aligned} \tag{12}$$

Figure 7 plots $\ln(\beta\, T_p^{-2})$ versus T_p^{-1} to estimate E_a and k_0 for 88 mass% TMCH that is reckoned using the ASTM E698 method. The E_a, k_0, and regression coefficient of pure TMCH were 147.4 kJ mol^{-1}, 3.994E+19 s^{-1} and 0.9957, respectively.

Reaction mixtures encountered in thermal analysis normally illustrate the complex mechanisms and the overall rate of reaction comprises multiple reaction schemes. In addition, the reaction is proposed to be *N*-th order for each compound, but autocatalytic reaction may sporadically encounter. The exothermic behaviors near the processing or storage temperature should be determined. The thermophysical parameters and the acid-catalyzed reaction models for TMCH and its mixture of four specific acids were estimated. In general processes, temperature control and reaction rate should be paid attention to the thermokinetic parameters of the operation and storage, as given in Table 3, to sustain a normal process operation.

Figures 8–12 show the comparisons of the DSC experiments and mathematical simulation results for heat

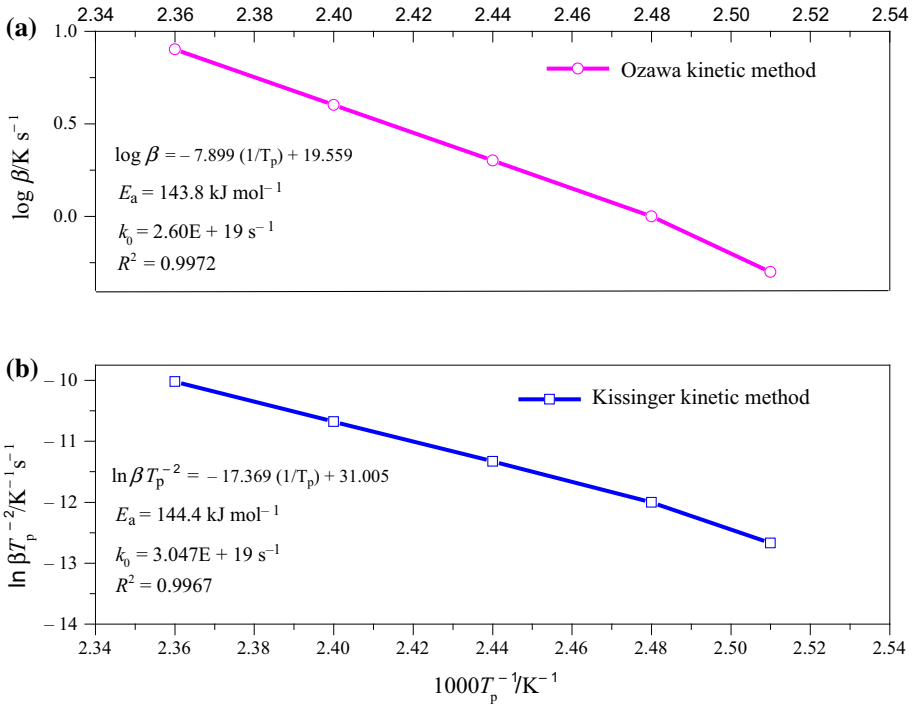

Fig. 7 Apparent activation energy (E_a) and rate constant (k_0) plot of 88.0 mass% TMCH evaluated by ASTM E691 including **a** Ozawa kinetic method and **b** Kissinger kinetic method, in which the peak temperature of thermal curve is varied with the heating rate changes

Table 3 Evaluated kinetics of the reaction model for estimating 88.0 mass% MCH with four specific acids, which include 6.0 N H_3PO_4, H_2SO_4, HNO_3, or HCl by TSS

Tested chemicals	Reaction profile	Parameter Unit	ln (k_0) ln/s^{-1}	E_a kJ mol^{-1}	n_1 Dimensionless	n_2***	z***	ΔH_d J g^{-1}
TMCH 88.0 mass%	*N*-th*	First stage	37	142	3.4	–	–	214
		Second stage	39	154	1.0	–	–	852
TMCH/H_3PO_4	*N*-th	First stage	9	55	0.8	–	–	229
		Second stage	44	171	0.6	–	–	518
		Third stage	23	98	0.8	–	–	654
TMCH/H_2SO_4	Auto.	First stage	51	54	3.1	0.7	0.0008	526
		Second stage	1	7	1.6	0.1	0.0017	392
		Third stage	7	18	0.8	0.1	0.17	202
TMCH/HNO_3	*N*-th/Auto.	First stage	139	459	3.0	0.8	0.0001	337
		Second stage	55	172	3.0	0.13	0.0052	606
		Third stage	9	49	1.9	0.71	0.0032	243
		Fourth stage	25	114	0.7	–	–	117
		Fifth stage	16	67	0.8	–	–	445
TMCH/HCl	Auto.**	First stage	121	348	6.8	0.18	0.0017	545
		Second stage	5	36	0.8	0.98	0.0025	70
		Third stage	11	48	1.8	1.7	0.0032	104
		Fourth stage	16	68	0.9	0.3	0.0032	376

*An *N*-th order reaction

**An autocatalytic reaction

***Strictly for the autocatalytic reaction

production and heat production rate at 4.0 °C min^{-1}. The simulation results of only TMCH under an isothermal condition conducted by TAM III combined with the *N*-th order reaction model are demonstrated in Fig. 8. As TMCH was added with 6.0 N H_2SO_4, three reaction stages are observed in Fig. 9. The reaction initiated at the second

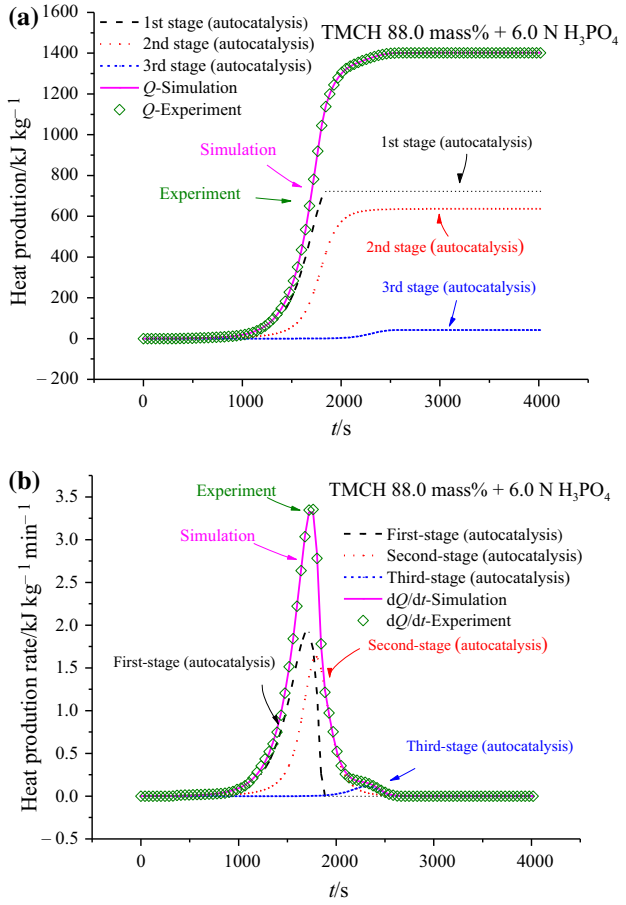

Fig. 8 Experimental and simulation results of **a** heat production and **b** heat production rate versus time for 88.0 mass% TMCH added with 6.0 N H_3PO_4

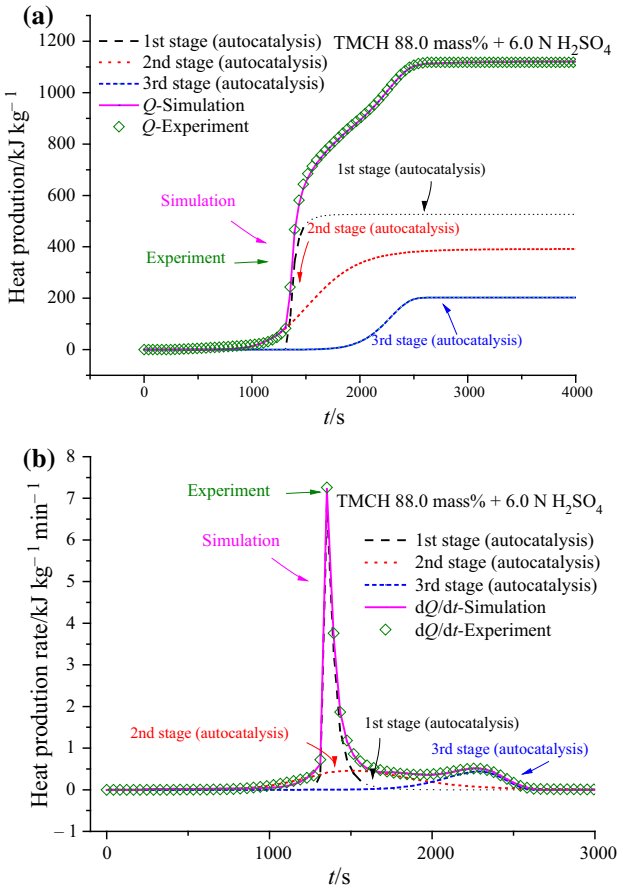

Fig. 9 Experimental and simulation results of **a** heat production and **b** heat production rate versus time for 88.0 mass% TMCH added with 6.0 N H_2SO_4

stage of the reaction. The reaction in the first stage appeared the maximum exothermic peak. Following the completion of first and second stages of the reaction, the third-stage decomposition was generated until the end of the overall reaction.

On the basis of the reaction mechanism under dynamic and isothermal conditions, the decomposition types can be classified as both *N*-th order reaction and autocatalytic reaction by evaluating the thermal curve, as shown in Fig. 10. By contrast, the thermal curves of TMCH with HNO_3 or HCl indicated that no decomposition or low reaction rate initially occurred (Figs. 10 and 11). As the reaction progressed, an autocatalytic product was produced that to accelerate the reaction and to reach the maximal reaction rate. TMCH reacting with HNO_3 showed the most complexity of reaction behavior including five exothermic stages. At the beginning of a reaction comprised of an autocatalysis reaction (second stage) and an *N*-th order reaction (fifth stage), the reaction rate of the second stage was faster than that of the fifth stage. After a period of time, the first-stage reaction occurred and generated the largest exothermic peak. The third and fourth stages were maintained unapparent exothermic types at the end of thermal decomposition. Therefore, the first, second, and fifth stages were the crucial stages of the TMCH-HNO_3 reaction that was determined to be the multiple forms of acid-catalyzed model.

The predominant reaction occurred at the second stage of the reaction; the heat production and heat production rate in the first stage of reaction were maintained at a low level. From the reactions of 88.0 mass% TMCH added with 6.0 N HCl, four-stage exothermic peaks can be clearly observed from the waveform of the heat production rate, as illustrated in Fig. 11. The reaction of the first stage has the principal heat production, and after predominant reaction of the first stage, the heat generation of 2nd to 4th stages increased during this exothermic reaction. The reactions of TMCH added with HNO_3 were observed when the maximal heating rate was employed at the onset of the reactions.

In the thermal analysis of TMCH reacting with H_3PO_4, both initial and second exothermic peaks exhibited the form of an autocatalytic reaction, as presented in Fig. 8. As

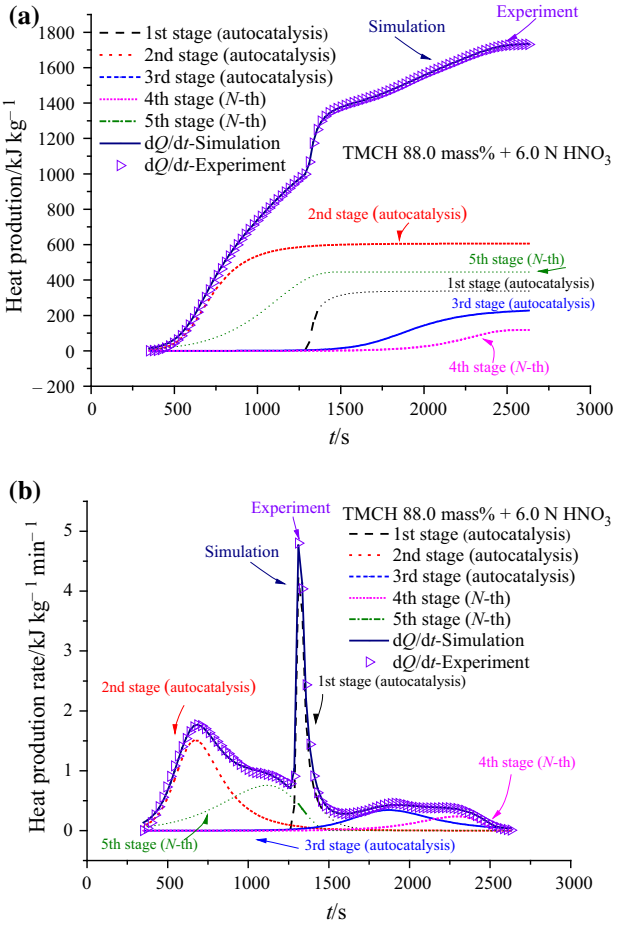

Fig. 10 Experimental and simulation results of **a** heat production and **b** heat production rate versus time for 88.0 mass% TMCH added with 6.0 N HNO_3

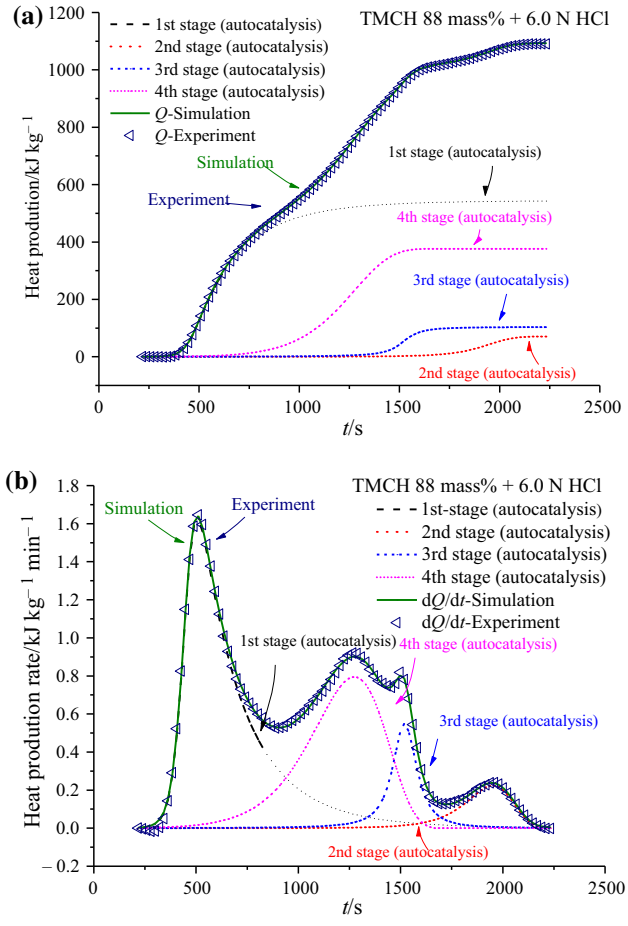

Fig. 11 Experimental and simulation results of **a** heat production and **b** heat production rate versus time for 88.0 mass% TMCH added with 6.0 N HCl

relevant to the *N*-th order reaction of TMCH, the TMCH-H_3PO_4 acid-catalyzed decomposition presented an autocatalytic effect, and the reactants were subsequently converted into products. As TMCH was added with 6.0 N H_3PO_4, three autocatalytic reactions appeared. During this thermal decomposition, the characteristic exothermic peaks were derived from the first and second stages of the reaction, and the third stage of the reaction emerged at the end of exothermic peak. Typically, a reaction has an initial reaction rate; however, as the reactants are being consumed, the products autocatalytically proceed the reaction. Under chemical processing conditions, autocatalytic reactions may be a safe consideration in process designs because of the induction of a further thermal runaway reaction [28, 29]. Therefore, the predictions of the temperature increase and reaction rate are important to ensure the process safety, specially coping with autocatalytic reactions [30].

Conclusions

Trace contaminants of ionizing acids could act as additional catalysts in the decomposition reaction of TMCH. For developing an inherently safer design, the thermally hazardous characteristics of TMCH and the characteristics when TMCH is mixed with H_3PO_4, H_2SO_4, HNO_3, or HCl were comprehensively recognized in this study. The thermophysical data and kinetic parameters of pure TMCH and its mixture of aforementioned strong acids were estimated that can classify the acid-catalyzed decomposition and assess the reaction model. If TMCH runs into acidic stimuli that is not only clearly altered the original reaction of TMCH but also shortened the induction time to cause the violent decomposition. The mixtures of TMCH with HCl or HNO_3 resulted in a higher reaction enthalpy in earlier temperatures and triggered advanced thermal runaway reactions by generating two prominent peaks during the decomposition. Thermal hazard characteristics received from TMCH added with H_2SO_4 or H_3PO_4 illustrated

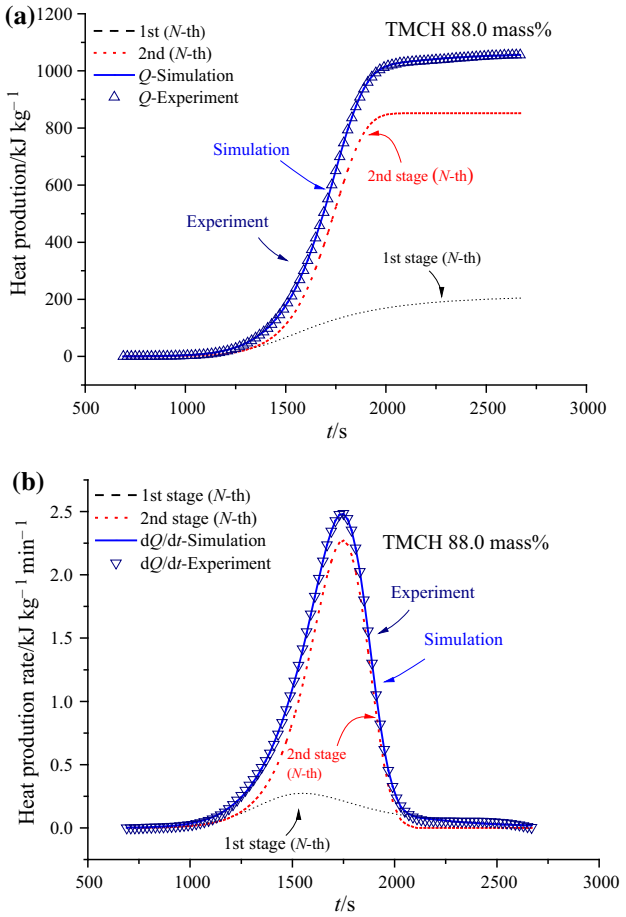

Fig. 12 Experimental and simulation results of **a** heat production and **b** heat production rate versus time for 88.0 mass% TMCH

exothermic trends of thermal decomposition similar in TMCH, but higher heat of decomposition of TMCH added with H_2SO_4 or H_3PO_4 has been seen.

On the basis of the DSC and TAM III analysis results, the apparent onset exothermic temperature of TMCH is near the ambient temperatures when TMCH is mixed with HNO_3 or HCl. The temperature and concentration of containment were the major factors to be accounted for processing or storing conditions. The heat of decomposition values for the various mixtures is in the following order: TMCH + H_2SO_4 > TMCH + HNO_3 > TMCH + HCl > TMCH + H_3PO_4 > TMCH. The initial exothermic peak exhibited features of an *N*-th order reaction, whereas the second peak was due to an autocatalytic reaction. Compared with all other mixtures, the mixture of TMCH and HNO_3 had the most complex profile and had the most complex *N*-th order and autocatalysis reactions. The kinetic variable must be taken into account in TMCH acid-catalyzed systems to establish the proper reaction kinetic models. This study employed a calorimetric approach and a reaction model to analyze the influence of impurities on a reaction including TMCH.

Acknowledgements The authors are grateful to the technical supports received from Mr. Chen-Rui Cao at YunTech.

References

1. Chen YL, Chou YP, Hou HY, I YP, Shu CM. Reaction hazard analysis for cumene hydroperoxide with sodium hydroxide or sulfuric acid. J Therm Anal Calorim. 2009;95(2):535–9.
2. Wu SH, Wang YW, Wu TC, Hu WN, Shu CM. Evaluation of thermal hazards for dicumyl peroxide by DSC and VSP2. J Therm Anal Calorim. 2008;93:189–94.
3. Chen JR, Wu SH, Lin SY, Hou HY, Shu CM. Utilization of microcalorimetry for an assessment of the potential for a runaway decomposition of cumene hydroperoxide at low temperatures. J Therm Anal Calorim. 2008;93:127–33.
4. Liu SH, Lin CP, Shu CM. Thermokinetic parameters and thermal hazard evaluation for three organic peroxides by DSC and TAM III. J Therm Anal Calorim. 2011;106:165–72.
5. Chen KY, Wu SH, Wang YW, Shu CM. Runaway reaction and thermal hazards simulation of cumene hydroperoxide by DSC. J Loss Prev Process Ind. 2008;21:101–9.
6. Wu LK, Chen KY, Cheng SY, Lee BS, Shu CM. Thermal decomposition of hydrogen peroxide in the presence of sulfuric acid. J Therm Anal Calorim. 2008;93:115–20.
7. Hou HY, Duh YS, Lin WH, Shu CM. Reactive incompatibility of cumene hydroperoxide added with alkaline solutions. J Therm Anal Calorim. 2006;85:145–50.
8. Duh YS, Wu XH, Kao CS. Hazard ratings for organic peroxides. Process Saf Prog. 2008;27:89–99.
9. Safety and handling of organic peroxides: a guide, organic peroxide producers safety division. Washington: The Society of the Plastics Industry, Inc.; 1999. http://www.plasticsindustry.org
10. Wang YW, Shu CM, Duh YS, Kao CS. Thermal runaway hazards of cumene hydroperoxide with contaminants. Ind Eng Chem Res. 2001;40:1125–32.
11. Wang YW, Liao MS, Shu CM. Thermal hazards of a green antimicrobial peracetic acid combining DSC calorimeter with thermal analysis equations. J Therm Anal Calorim. 2015;119:2257–67.
12. Wang YW. Evaluation of self-heating models for peracetic acid using calorimetry. Process Saf Environ. 2018;113:122–31.
13. Tseng JM, Lin CP, Huang ST, Hsu J. Kinetic and safety parameters analysis for 1,1,-di-(*tert*-butylperoxy)-3,3,5-trimethylcyclohexane in isothermal and non-isothermal conditions. J Hazard Mater. 2011;192:1427–36.
14. Tseng JM, Lin JZ, Lee CC, Lin CP. Prediction of TMCH thermal hazard with various calorimetric tests by green thermal analysis technology. AIChE J. 2012;58(12):3792–8.
15. Chen WT, Chen WC, You ML, Tsai YT, Shu CM. Evaluation of thermal decomposition phenomenon for 1, 1-bis (*tert*-butylperoxy)-3,3,5-trimethylcyclohexane by DSC and VSP2. J Therm Anal Calorim. 2015;122:1125–33.
16. Hsueh KH, Chen WC, Chen WT, Shu CM. Thermal decomposition analysis of 1,1-bis(*tert*-butylperoxy)cyclohexane with sulfuric acid contaminants. J Loss Prevent Proc Ind. 2016;40:357–64.
17. Chen WC, Chen WT, Wang YW, Chiu CW, Shu CM. Effects of mixing metal ions for the thermal runaway reaction of TMCH. J Therm Anal Calorim. 2014;118:1003–10.

18. Huang AC, Chen WC, Huang CF, Zhao JY, Deng J, Shu CM. Thermal stability simulations of 1,1-bis(*tert*-butylperoxy)-3,3,5 trimethylcyclohexane added with metal ions. J Therm Anal Calorim. 2017;130:949–57.
19. Yeh CT, Chen WC, Shu CM. Thermal hazard assessment of TMCH added with inorganic acids. MATEC Web Conf. 2018;169:1–9.
20. Lin SY, Tseng JM, Lin YF, Huang WT, Shu CM. Comparison of thermal polymerization mechanisms for α-methylstyrene and trans-β-methylstyrene. J Therm Anal Calorim. 2008;93:257–67.
21. Rodríguez-de-Rivera M, Socorro F. Signal processing and uncertainty in an isothermal titration calorimeter. J Therm Anal Calorim. 2007;88:745–50.
22. Chen HX, Liu NA. A procedure to approximate the generalized temperature integral. J Therm Anal Calorim. 2007;90:449–52.
23. Tseng JM, Liu MY, Chen SL, Hwang WT, Gupta JP, Shu CM. Runaway effects of nitric acid on methyl ethyl ketone peroxide by TAM III test. J Therm Anal Calorim. 2009;96:789–93.
24. Ho TC, Duh YS, Chen JR. Case studies of incidents in runaway reactions and emergency relief. Process Saf Prog. 1998;17:259–62.
25. Kossoy AA, Benin AI, Akhmetshin YG. An advanced approach to reactivity rating. J Hazard Mater. 2005;118:9–17.
26. Kossoy AA, Akhmetshin YG. Identification of kinetic models for the assessment of reaction hazards. Process Saf Prog. 2007;26:209–20.
27. ASTM E698-18. Standard test method for kinetic parameters for thermally unstable materials using differential scanning calorimetry and the Flynn/Wall/Ozawa method. West Conshohocken: ASTM International; 2018.
28. Andreozzi A, Buonomo B, Manca O. Numerical study of natural convection in vertical channels with adiabatic extensions downstream. Numer Heat Transfer Part A. 2005;47:741–62.
29. Neylon MK, Savage PE. Analysis of non-isothermal heterogeneous autocatalytic reactions. Chem Eng Sci. 1996;51:851–8.
30. Parulekar SJ. Modal analysis and optimization of isothermal autocatalytic reactions. Chem Eng Sci. 1998;53:2379–94.